Non-uniform Torsional Eigenmodes of FGM Beams

Justin Murin, Mehdi Aminbaghai, Juraj Hrabovsky, Vladimir Kutis, Stephan Kugler, and Juraj Paulech

Abstract In this contribution, which is an extension of our research (Murin et al. in J Eng Struct 175:912–925, 2018 [6]), the influence of spatially varying material properties on torsional eigenvibration of the FGM beams is investigated. Based on the semi-analytical solution of the fourth-order differential equation for non-uniform torsion, the local finite element equations of the twisted FGM beam are established, considering the non-uniform torsion with the effect of warping and secondary deformations due to the angle of twist. The warping part of the first derivative of the twist angle caused by the bimoment is considered as an additional degree of freedom at the beam nodes. The focus of the numerical investigation, with consideration of the warping and Deformation Effect due to the Secondary Torsional Moment (STMDE), is on modal analysis of straight cantilever FGM beams with doubly symmetric closed cross-sections. The influence of the spatial variation of the material properties on the eigenfrequencies is investigated. The obtained results are compared with the ones calculated by a very fine mesh of standard solid finite elements.

J. Murin (✉) · J. Hrabovsky · V. Kutis · J. Paulech
Slovak University of Technology in Bratislava, Bratislava, Slovakia
e-mail: justin.murin@stuba.sk

J. Hrabovsky
e-mail: juraj.hrabovsky@stuba.sk

V. Kutis
e-mail: vladimir.kutis@stuba.sk

J. Paulech
e-mail: juraj.paulech@stuba.sk

M. Aminbaghai
Vienna University of Technology, Vienna, Austria
e-mail: mehdi.aminbaghai@tuwien.ac.at

S. Kugler
University of Applied Sciences Wiener Neustadt, Wiener Neustadt, Austria
e-mail: kugler@fhwn.ac.at

E. J. Sapountzakis et al. (eds.), *Proceedings of the 14th International Conference on Vibration Problems*, Lecture Notes in Mechanical Engineering,
https://doi.org/10.1007/978-981-15-8049-9_17

Keywords FGM beams · Spatial variation of material properties · Non-uniform torsion · Modal analysis

1 Introduction

Novel engineering technologies face the challenge of answering increasingly complex questions about the functionality of the developed systems. In material science, one of the ground-breaking technologies is Functionally Graded Materials (FGMs), where the material properties are graded in one, two or three directions. Fabrication of such materials is complicated, but progress in this area has been significant in recent years. From the macroscopic point of view, FGMs are isotropic at each material point, but the material properties can vary continuously or discontinuously in one, two, or three directions. The variation of the macroscopic material properties can be caused by varying the volume fraction of the constituents or their material. Important structural components made of FGMs are beams. Thin-walled beams play an important role not only in structural applications, but also in thermal, thermo-structural or electric-thermal-structural systems (e.g. MEMS sensors and actuators), and in mechatronics. In all applications, new materials, such as FGMs, can greatly improve the efficiency of engineering systems. From this point of view, a development of new approaches for mechanical analysis of FGM structures is straightforward.

Beam structures are often exposed to time-dependent loads. A comprehensive overview of the literature, dealing with the issue of non-uniform torsion of the material homogeneous beams can be found, e.g., in [1, 2]. Commercial FEM codes allow performing modal and transient dynamic analysis by 3D finite beam elements with and without consideration of the warping effect [3–5]. For torsion, very often an improved Saint-Venant theory is used and special mass matrices are proposed. In general, the bicurvature is chosen as an additional warping degree of freedom, and the STMDE is not considered. As stated in [4], for solid and closed thin-walled sections, standard finite beam elements can be used without significant error. However, for open thin-walled sections, warping finite beam elements should be used [5]. A common feature of the cited articles is that constant material properties of the twisted beams are assumed. In the literature, there is very hard to find papers which deal with uniform and non-uniform torsion of FGM beams with spatially varying material properties. In [6], the beam finite element for Saint-Venant and non-uniform torsion modal analysis of the FGM beams with longitudinal variation of material properties is presented. As shown, the longitudinal variation of material properties influences the eigenfrequencies of the thin-walled beams of open cross-section very strong. This effect has been shown also by the closed cross-section beams. The new contribution is an extension of the paper [6]. Here, the results of the non-uniform modal analysis of the FGM beams with continuously varying material properties in the longitudinal, transversal and lateral direction are presented. The spatial variability of the material properties in the real beam are homogenized by the Multilayer (MLM) [9] and the Reference Beam Methods (RBM) [8] into constant or longitudinally linear varying

effective properties. In Sect. 2, the differential equation for non-uniform torsional deformations of the FGM beam with longitudinal variation of the effective material properties, including the inertial line moments, is presented. The part of the bicurvature caused by the bimoment is taken into account as the warping degree of freedom, and the STMDE is also considered. A general semi-analytical solution of the differential equation is shortly described, from which the finite element equations of the straight warping torsion (WT) finite beam elements with two-nodes are obtained. Omitting the external load, the Finite Element Method (FEM) equations for torsional natural free vibrations are obtained. The equations are then used for non-uniform torsional modal analysis of the FGM beams with spatially varying material properties (polynomial variation in the longitudinal direction and symmetric variation in the lateral and transversal direction). In Sect. 3, the methods are presented for homogenization of the spatially varying material properties into the longitudinally varying as the effective elastic properties and the mass density. If the material properties vary symmetrically according to the lateral and transversal central axis, then the effective properties are constant in the longitudinal direction. Section 4 contains the numerical investigation. The results from modal analysis of cantilever FGM beams with spatially varying material properties are presented and compared with results obtained from commercial FEM codes. The effect of the spatially varying material properties is evaluated and discussed. A final assessment of the proposed method is contained in the Conclusions.

2 Differential Equation for Non-uniform Torsion Eigenvibration and Its Solution

Figure 1 refers to determination of the eigenvibrations due to non-uniform torsion. It shows the torsional moment $M_T(x)$, representing the sum of the primary torsional moment $M_{Tp}(x)$ and the secondary torsional moment $M_{Ts}(x)$, and the bimoment $M_\omega(x)$ according to the formulation in the framework of the Transfer Matrix Method (TMM). This figure also shows the angle of twist $\psi(x)$, corresponding to $M_{Tp}(x)$. It represents the sum of the angle of twist, resulting from the primary deformation, $\psi'_M(x)$ and from the secondary deformation, $\psi'_S(x)$.

Figure 2 illustrates the finite beam element. It is loaded by the equivalent inertial torsional line moment $\omega^2 I_p \rho(x)\psi(x)$, the equivalent inertial line bimoment $\omega^2 I_\omega \rho(x)\psi'_M(x)$, where I_ω stands for the warping constant, and the torsional line moment $m_T(x)$, which is equal to zero for modal analysis. The circular frequency is

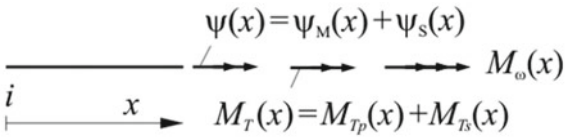

Fig. 1 Non-uniform torsion: torsional moments, bimoment, and angles of twist

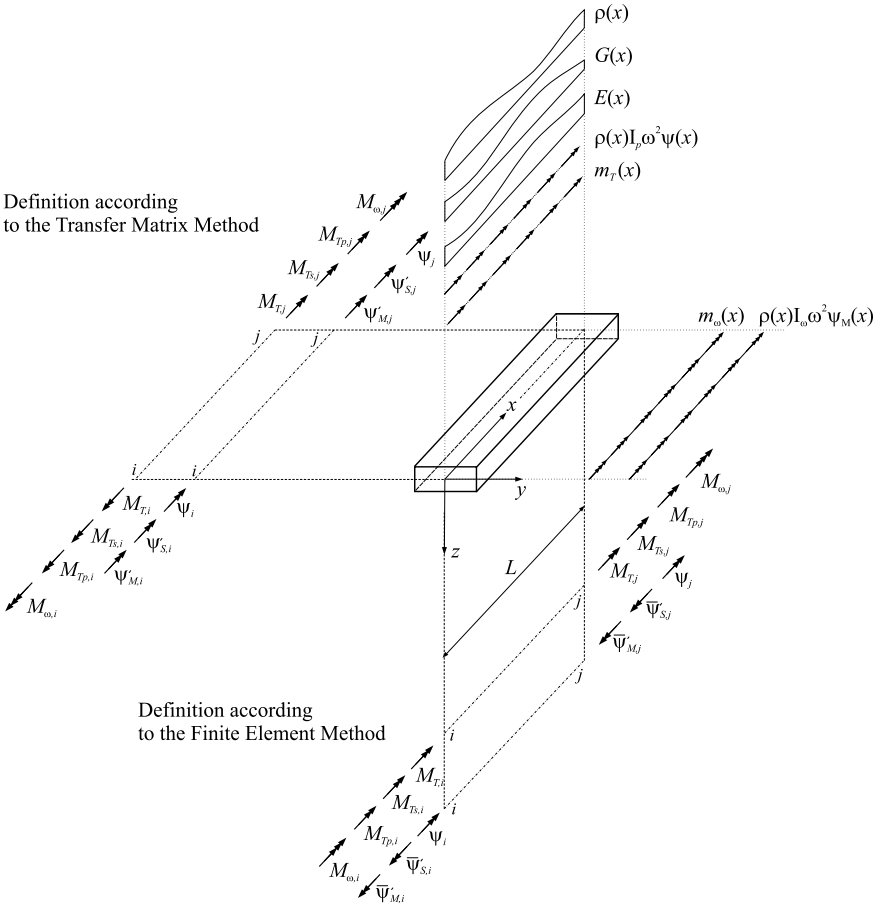

Fig. 2 Positive orientation of the moments and rotation angles at element nodes for the TMM and the FEM

ω and I_p is the polar quadratic moment of area. These line moments represent the static equivalent of the respective dynamic action. In the following, the equilibrium equations will be formulated. They are obtained as

$$M_T'(x) = -m_T(x) - \omega^2 I_p \rho(x) \psi(x), \tag{1}$$

where $m_T(x) = \sum_{k=0}^{\max k} \eta_{m_T,k} x^k$ is the polynomial representation of the torsion moment with the parameters $\eta_{m_T,k}$, and

$$\begin{aligned} M_\omega'(x) &= M_T(x) - M_{Tp}(x) + m_\omega(x) + \omega^2 I_\omega \rho(x) \psi_M'(x) \\ &= M_{Ts}(x) + m_\omega(x) + \omega^2 I_\omega \rho(x) \psi_M'(x), \end{aligned} \tag{2}$$

where $m_\omega(x) = \sum_{k=0}^{\max k} \eta_{m_\omega,k} x^k$ is the polynomial representation of the warping moment with the parameters $\eta_{m_\omega,k}$, and

$$M_T(x) = M_{Tp}(x) + M_{Ts}(x). \tag{3}$$

According to [6, 7],

$$\psi''_M(x) = -\frac{M_\omega(x)}{E(x)I_\omega} \tag{4}$$

And

$$\psi'(x) = \psi'_M(x) + \psi'_S(x) \tag{5}$$

with

$$\psi'(x) = \frac{M_{Tp}(x)}{G(x)I_T} \tag{6}$$

and

$$\psi'_S(x) = \frac{M_{Ts}(x)}{G(x)I_{Ts}}, \tag{7}$$

where I_{Ts} denotes the secondary torsion constant and $E(x)$ and $G(x)$ stand for the longitudinally varying effective elasticity modulus and shear modulus, respectively.

As detailed in [6], the following homogeneous differential equation of fourth order with variable parameters η for angle of rotation $\psi(x)$ is obtained:

$$\eta_4(x)\psi''''(x) + \eta_3(x)\psi'''(x) + \eta_2(x)\psi''(x) + \eta_1(x)\psi'(x) + \eta_0(x)\psi(x) = 0. \tag{8}$$

Here and in the following, $' := d/dx$. The semi-analytical solution of the differential Eq. (8) can be written as follows:

$$\psi(x) = b_0(x)\psi_i + b_1(x)\psi'_i + b_2(x)\psi''_i + b_3(x)\psi'''_i. \tag{9}$$

In (9), $b_0(x)$, $b_1(x)$, $b_2(x)$, $b_3(x)$ denote the transfer functions and ψ_i, ψ'_i, ψ''_i, ψ'''_i stand for the integration constants at the starting point i, see Fig. 1, (e.g. $\psi_i = \psi(x)$ for $x = 0$, etc.…). They can be calculated numerically [1]. Using appropriate mathematical operations [6], then from the transfer matrix method relations the finite element equations for non-uniform torsion (in particular, for free torsional vibrations) were established. Considering the definitions of positive quantities in the framework of the FEM, resulting in $\bar{M}_{T,i} = -M_{T,i}$, $\bar{M}_{\omega,i} = -M_{\omega,i}$, $\bar{\psi}'_{M,i} = -\psi'_{M,i}$, and $\bar{\psi}'_{M,j} = -\psi'_{M,j}$, the finite element equations read:

$$\begin{bmatrix} \bar{M}_{T,i} \\ \bar{M}_{\omega,i} \\ M_{T,j} \\ M_{\omega,j} \end{bmatrix} = \begin{bmatrix} B_{1,1} & B_{1,2} & B_{1,3} & B_{1,4} \\ B_{2,1} & B_{2,2} & B_{2,3} & B_{2,4} \\ B_{3,1} & B_{3,2} & B_{3,3} & B_{3,4} \\ B_{4,1} & B_{4,2} & B_{4,3} & B_{4,4} \end{bmatrix} . \begin{bmatrix} \psi_i \\ \bar{\psi}'_{M,i} \\ \psi_j \\ \bar{\psi}'_{M,j} \end{bmatrix} + \begin{bmatrix} F_1 \\ F_2 \\ F_3 \\ F_4 \end{bmatrix}. \tag{10}$$

The kinematic and kinetic variables at node i (for $x = 0$) are denoted by the index i in (10). By setting $x = L$ in this relation, the dependence of the nodal variables at node j on the nodal variables at node i is obtained. A detailed description of the matrix coefficients in (10) is presented in [6]. The local finite element matrix $\boldsymbol{B}$ in (10) is symmetric. It consists of the stiffness matrix $\boldsymbol{K}$ and the consistent mass matrix $\boldsymbol{M}$ (11):

$$[\mathbf{B}] = \left[\mathbf{K} - \omega^2 \mathbf{M}\right]. \tag{11}$$

The circular eigenfrequency is denoted by the symbol ω. In modal analysis of a single beam, an eigenvalue problem must be solved. For given longitudinally varying effective material properties and the boundary conditions, the value of the circular frequency ω is increased until the determinant of the finite element matrix becomes zero. The respective circular frequency is the natural circular frequency, from which the natural frequency (eigenfrequency) can be calculated. Further, the mode shape can be calculated by the transfer relation [6]. The aforementioned finite element will be used in the following chapters to solve the eigenfrequencies of FGM beams with the spatially variation of material properties after their homogenization to longitudinal variation.

3 Homogenization of the Spatially Varying Material Properties

The stiffness matrix $\boldsymbol{K}$ in (11) contains: the bimoment stiffness $E(x)I_\omega$ that is a product of the effective elasticity modulus $E(x)$ and the warping constant I_ω; the primary torsional stiffness $G(x)I_T$ that is a product of the effective shear modulus $G(x)$ and the torsion constant I_T, and the secondary torsional stiffness $G(x)I_{Ts}$ that is a product of the effective shear modulus $G(x)$ and the secondary torsion constant I_{Ts}. The mass matrix $\boldsymbol{M}$ in (4) contains the inertial moments: $\rho(x)I_p$ and $\rho(x)I_T$ and $\rho(x)I_\omega$ and $\rho(x)I_{Ts}$. There, $\rho(x)$ stands for the effective mass density and I_p stands for the polar quadratic moment of area. All the geometrical parameters of the cross-sectional area are considered constant and independent from the material properties variation. They are calculated by the Thin Tube Theory (TTT) [7], or numerically by the FEM [3]. Homogenization of the spatially varying material properties for the examples presented in the Sect. 4 are done by the above mentioned MLM [9]. For results comparison, the same examples were solved using the effective material properties that are obtained by the Reference Beam Method (RBM) [8].

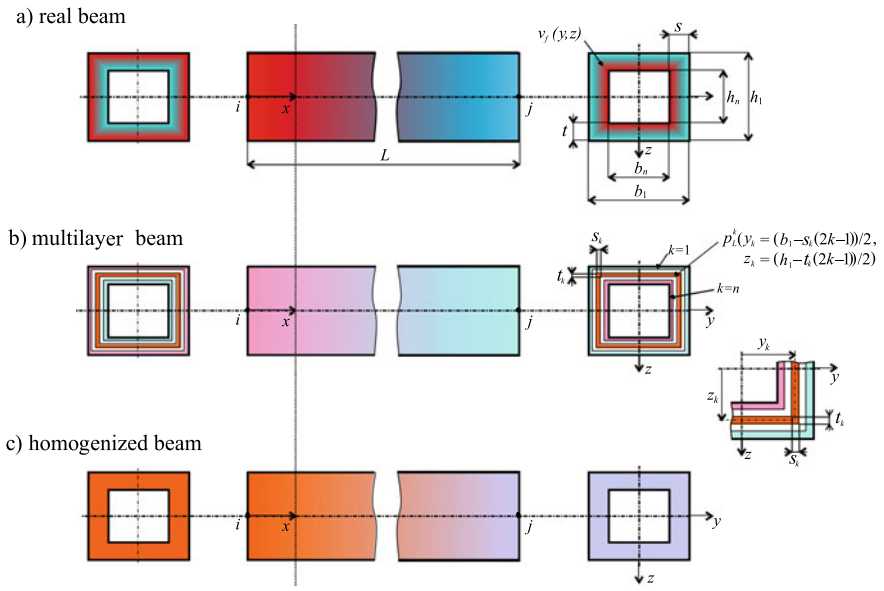

Fig. 3 A straight FGM beam of the hollow cross-section

The MLM, which is shortly described in the following subchapter, is applicable for the doubly symmetric cross-sections (rectangle, I-profile, hollow cross-section) with symmetric variation of the material properties in the lateral and transversal directions of the cross-section. A division into the layers depends on the shape of the cross-section. As an example, the straight FGM beam of the rectangular hollow cross-section is showed in Fig. 3.

According to Fig. 3a, the real material properties are: $E(x, y, z)$ is the elastic modulus, $\nu(x, y, z)$ is the Poisson's ratio, $G(x, y, z) = E(x, y, z)/(2(1 + \nu(x, y, z)))$ is the shear modulus and $\rho(x, y, z)$ is the mass density: $(x \in \langle 0, L\rangle, y \in \langle \pm h_n/2, \pm h_1/2\rangle, z \in \langle \pm b_n/2, \pm b_1/2\rangle)$. As shown in Fig. 3b, the hollow cross-section A at a distance x is divided to the k hollow layers with the cross-sectional area A_k, and with the constant elasticity modulus, $E_k(x)$, and the mass-density $\rho_k(x)$.The effective homogenized material properties in Fig. 3c, for example the elastic modulules, are calculated under assumption, that the relevant stiffness of the homogenized beam is equal to the stiffness of the real beam virtually divided into the hollow parts. Thus, we get the effective elastic modulus for axial loading

$$E(x) = \frac{\sum_{k=1}^{n-1} E_k(x) A_k}{A}. \tag{12}$$

There, $E_k(x) = [E(x, y, z)]_{\substack{y=y_k \\ z=z_k}}$ is the elasticity modulus of the kth layer, $(k \in \langle 1, \ n\rangle)$, and n is the number of layers, and A is the cross-sectional area. The

effective elastic modulus for torsion reads,

$$G(x) = \frac{\sum_{k=1}^{n} G_k(x) I_{T,k}}{I_T}, \tag{13}$$

with $G_k(x) = [G(x, y, z)]_{\substack{y=y_k \\ z=z_k}}$. The torsion constant of the kth hollow part ($k \in \langle 1, \ n \rangle$) can be evaluated as

$$I_{T,k} = \frac{2(b_1 - s_k(2k-1))^2 (h_1 - t_k(2k-1))^2}{\frac{(b_1 - s_k(2k-1))}{t_k} + \frac{(h_1 - t_k(2k-1))}{s_k}}. \tag{14}$$

The effective mass density for torsion is

$$\rho(x) = \frac{\sum_{k=1}^{n} \rho_k(x) I_{p,k}}{I_p}, \tag{15}$$

with $\rho_k(x) = [\rho(x, y, z)]_{\substack{y=y_k \\ z=z_k}}$. The polar quadratic moment I_p of the cross-section is chosen for the effective mass-density calculation. If the material properties in the real beam vary only in the lateral and transversal direction, constant effective material properties in the longitudinal direction are obtained from the above equations. However, it should be noted that it may be useful to calculate the effective mass density for all types of inertia moments, which were mentioned at the beginning of this chapter. This is not reflected in this contribution for the MLM homogenzation, but we will address it in our next work. An advantage of the MLM is their simplicity. The RBM homogenization method will be described in more detail in [8]. By this method, unlike the MLM, the bimoment and torsional stiffness of the heterogeneous cross-section is homogenized as a product of the elasticity modulus and the relevant cross-sectional characteristic.

4 Numerical Experiments

Example 1 FGM cantilever beam of the rectangular cross-section.

A clamped FGM beam is considered as shown in Fig. 4. Its rectangular cross-section is constant with the height $h = 0.005$ m and width $b = 0.01$ m. The length of the beam is $L = 0.1$ m. The local coordinate system is denoted with the axis x, y, and z. The material of the beam consists of two components: Aluminium Al6061-TO—denote with the index m and Titanium Carbide TiC—denoted with the index f. The material properties of the components are assumed to be constant and their values are: Aluminium Al6061-TO—the elastic modulus $E_m = 69.0$ GPa, the mass density $\rho_m = 2700$ kgm^{-3}, the Poisson's ratio $\nu_m = 0.33$; Titanium carbide TiC—the elastic modulus $E_f = 480.0$ GPa, the mass density $\rho_f = 4920$ kgm^{-3}, the Poisson's ratio $\nu_f = 0.20$. The axial, bending and uniform-torsion eigenfrequencies

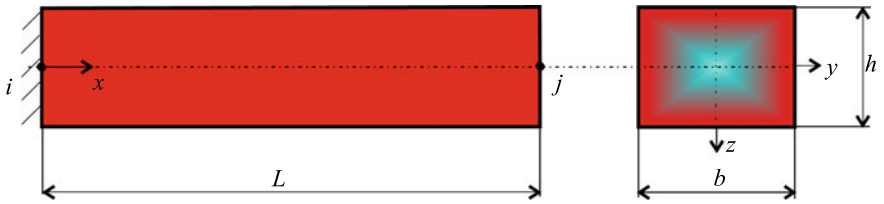

Fig. 4 A straight FGM beam of the rectangular cross-section with the varying material properties in two directions

were presented in [9]. In the following, the non-uniform torsional modal analysis was performed using the finite element presented in the Sect. 2. As shown in [1], an effect of the STMDE is not significant in modal analysis of the rectangular cross-sectional beam that is made of the homogeneous material. From this point of view, this effect will be neglected also in following modal analysis of the FGM beams with the rectangular cross-section.

The volume fraction of the reinforcing constituent varies in the y and z direction linearly and symmetrically according to the x-y and x-z planes: $\left[v_f(y,z)\right]_{\substack{y=0\\z=0}} = 0$, $\left[v_f(y,z)\right]_{\substack{y=\pm h/2\\z=\pm b/2}} = 1$—the core of the beam is made from the Aluminium and linearly varies to the edges that are made from the Titanium carbide. Using the MLM with 20 layers, the constant homogenized effective properties were obtained in the local x -direction of the beam: the elastic modulus for axial loading $E = 342.8$ GPa, the shear modulus for torsion $G = 162.2$ GPa, and the mass density for torsion $\rho = 4473.13$ kgm^{-3}, are calculated using Eqs. (5–7). The relevant cross-sectional parameters were calculated by ANSYS [3]: $A = 0.5 \times 10^{-4}$ m^4, $I_p = 5.208 \times 10^{-10}$ m^4, $I_\omega = 3.175 \times 10^{-16}$ m^6, $I_T = 2.885 \times 10^{-8}$ m^4.

Using the RBM [8], by which directly the bimoment stiffness and the torsional shear stiffness were homogenized, the following results were obtained: $EI_\omega = 1.3427 \times 10^{-4}$ Nm^4, $GI_T = 42.254$ Nm^2. The effective mass-density, which is calculated by MLM (which is equal to 4473.13 kgm^{-3}), is used also in the solved case with the RBM homogenization.

The first 4 torsional eigenfrequencies are evaluated using the new warping torsion FGM beam finite element (denoted in Table 1 by the $\mathrm{WT_m}$ for MLM homogenization and by the $\mathrm{WT_k}$ for RBM homogenization)—all the calculations are done with

Table 1 The Eigenfrequencies of the FGM beam of the rectangular cross-section

Eigenfrequency (Hz)	$\mathrm{WT_m}$	$\mathrm{WT_k}$	SOLID186	difm (%)	difk (%)
First	11,341	10,844	11,214	1.1	3.2
Second	34,080	32,613	33,661	1.2	3.1
Third	56,984	54,623	56,167	1.4	2.7
Fourth	80,160	77,024	78,769	1.7	2.2

our method that is implemented into MATHEMATICA software [10]. The eigenfrequency problem is also solved using a very fine mesh of 32,000 of SOLID186 elements [3]. In the ANSYS solution, the real distribution of the material properties has been used in the SOLID186 finite element model. It has to be pointed out that the entire structure is discretized using only one of our proposed beam finite elements. The average percent differences between the eigenfrequencies calculated by our warping torsion element, (using MLM (difm) and RBM (difk) homogenization), and by the SOLID186 elements are also shown in Table 1. As shown in Table 1, the percent differences of our results, considering both the homogenization methods, are acceptable compared to the SOLID186 FE results. A minor deviation was obtained with MLM homogenization. The high efficiency of our method is obvious since our results are evaluated using only one of our warping torsion beam elements compared to the large number of elements used in the continuum mesh.

Example 2 A FGM cantilever beam of the rectangular cross-section with variation of the material properties in three directions.

The cantilever beam is shown in Fig. 5. The geometry and material properties of the FGM constituents are the same as they are in the Example 1. At node i is $\left[v_{fi}(y,z)\right]_{\substack{y=0\\z=0}} = 1$, $\left[v_{fi}(y,z)\right]_{\substack{y=\pm h/2\\z=\pm b/2}} = 0$ and then vary continuous linearly in the longitudinal direction to the constant value at node j ($v_{fj} = 1$).

Using MLM with $n = 20$ layers the effective elastic modulus for axial loading $E(x)$, the torsional shear modulus $G(x)$, and mass density $\rho(x)$ for tension and $\rho(x)$ for torsion are evaluated as

$E(x) = 342.109 - 2731.095x$ GPa; $G(x) = 162.233 - 1362.936x$ GPa; $\rho(x) = 4468.34 - 17683.43x$ kgm^{-3}.

The first four eigenfrequencies f (Hz) are evaluated as shown in Table 2. It was used in only one of our proposed finite elements and the MLM homogenization

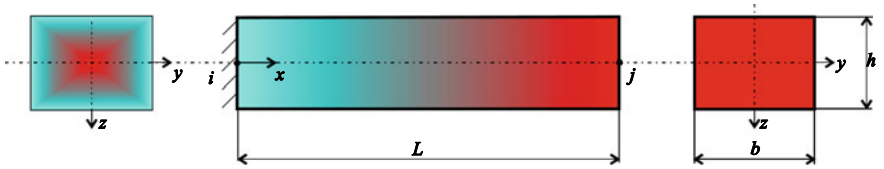

Fig. 5 A straight FGM beam of the rectangular cross-section with the varying material properties in three directions

Table 2 The Eigenfrequencies of the FGM beam for Example 2

f (Hz)	SOLID186	WTm	Δ%
First	10,926	10,002	8.45
Second	26,718	25,133	5.9
Third	43,568	41,248	5.3
Fourth	61,444	57,624	6.2

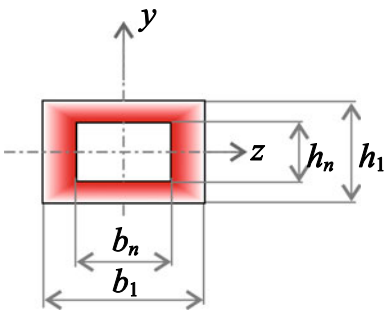

Fig. 6 The rectangular hollow cross-section with the varying material properties in two directions

will be applied. The same problem is solved using a very fine mesh—32,000 of SOLID186 elements of the FEM program ANSYS. By the SOLID186 FE model, the real distribution of the material properties has been assigned to relevant finite elements. The results of ANSYS as well as the results of the WTm are presented in Table 2. The average relative difference Δ (%) between eigenfrequencies calculated by our method and the ANSYS solution is evaluated.

Table 2 shows larger percent deviation of the compared frequencies as it was in Example 1. Nevertheless, these results can be considered acceptable.

Example 3 A FGM cantilever beam of the rectangular hollow cross-section with variation of the material properties in two directions.

In this example, the results of modal analysis of the cantilever FGM beam with rectangular hollow cross-section will be presented. A geometry of the cross-section, Fig. 6, is given by $h_1 = 0.005$ m, $h_n = 0.00375$ m, $b_1 = 0.01$ m, $b_n = 0.0075$ m. The length of the cantilever beam is $L = 0.1$ m.

The cross-sectional characteristics, which were calculated by the TTT, are: the cross-sectional area is $A = 2.1875 \times 10^{-5}$ m^2, the second moments of area are $I_y = 7.12077 \times 10^{-11}$ m^4 and $I_z = 2.84831 \times 10^{-10}$ m^4, the polar moment of area is $I_p = I_y + I_z = 3.56038 \times 10^{-10}$ m^4 and the torsion constant is $I_T = 1.6748 \times 10^{-10}$ m^4. The warping constant is $I_\omega = 2.40426 \times 10^{-16}$ m^6 and the secondary torsion constant is $I_{Ts} = 7.1777 \times 10^{-11}$ m^4.

The material of the beam consists of two components: Aluminium Al6061-TO—denote with index m and Titanium carbide TiC—denoted with index f. The material properties of the components are assumed to be constant and their values are the same as the ones used in the Examples 1 and 2. The TiC volume fraction varies in the y and z direction linearly and symmetrically according to the $x - y$ and $x - z$ planes: $\left[v_f(y,z)\right]_{\substack{y=\pm h_n/2 \\ z=\pm b_n/2}} = 0$, $\left[v_f(y,z)\right]_{\substack{y=\pm h_1/2 \\ z=\pm b_1/2}} = 1$—the inner edges of the cross-sectional area are made of the pure Al6061-TO—and the outer cross-section edges are made of the pure TiC. Constant effective material properties are considered in the x-direction. Using the MLM with 20 layers, the effective elastic modulus for axial loading $E = 284.261$ GPa, the torsional shear modulus $G = 124.685$ GPa, and the mass density $\rho = 3965.643$ kgm^{-3} for torsion, were calculated.

Table 3 The Eigenfrequencies of the FGM beam for Example 2

f (Hz)	SOLID186	WTm	difm (%)	WTk	difk (%)
First	9788	9673	1.2	10,117	3.3
Second	30,928	29,078	5.9	30,428	1.6
Third	49,124	48,656	0.9	50,950	3.7
Fourth	68,756	68,498	3.7	71,728	4.3

Using the RBM [8], by which the bimoment stiffness and the torsional shear stiffness were directly homogenized, the following results were obtained: $E_\omega I_\omega = 8.9877 \times 10^{-5}$ Nm^4, $G_T I_T = 22.7956$ Nm^2. The effective mass-density, which is calculated by the MLM (which is equal to 4473.13 kgm^{-3}), is used also in the solved case with the RBM homogenization.

The FGM clamped beam was studied by modal analysis. The first four torsional eigenfrequencies f (Hz) are given in Table 3 using our only one FGM beam finite element with the homogenized material properties. The STMDE was considered as well.

For comparison purposes, the same problem is solved using a very fine mesh—21,600 of SOLID186 elements of the FEM program ANSYS. The average percent differences between the eigenfrequencies calculated by our warping torsion element, (using MLM (difm) and RBM (difk) homogenization), and by the SOLID186 elements are also shown in Table 3. A good agreement of the results was obtained. The larger difference in the 2nd and 3rd eingefrequencies may be due to distortion of the cross-section that is not taken into account in our method. In Fig. 7, the 1st and 3rd torsional mode of the FGM cantilever beam are displayed.

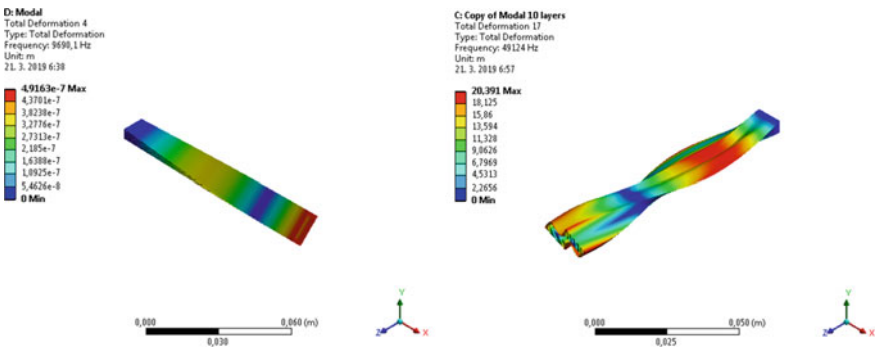

Fig. 7 The 1st and 3rd mode

5 Conclusions

In the contribution, results of the non-uniform modal analysis of the cantilever FGM beams with the rectangular and hollow cross-section are presented. The continuously varying material properties in two or three directions were homogenized by the MLM and RBM. The non-uniform torsion modal analysis was done by the author's warping torsion beam finite element with the four degrees of freedom. Effect of the distortion of the cross-sections was not considered. The part of the bicurvature caused by the bimoment was used as the warping degree of freedom. Only one of the beam element was used in the computational modelling of the cantilever FGM beams. For results comparison, the modal analyses by the SOLID186 FE were performed. A very fine mesh of the finite element was used for modelling of the FGM beams with the real spatial distribution of the material properties. The obtained results agree well with the results from finite solid elements. As expected, the spatially varying material properties influence the natural vibration significantly.

Acknowledgements The authors gratefully acknowledge financial support by the Slovak Grant Agency of the project VEGA No. 1/0102/18 and VEGA No. 1/0081/18.

References

1. Murin J, Aminbaghai M, Hrabovsky J, Mang HA (2016) Torsional warping eigenmodes including the effect of the secondary torsion moment on the deformations. J Eng Struct 106:299–316. https://doi.org/10.1016/j.engstruct.2015.10.022
2. Dikaros IC, Sapountzakis EJ, Argyridi AK (2016) Generalized warping effect in the dynamic analysis of beams of arbitrary cross sections. J Sound Vib 369:119–146. https://doi.org/10.1016/j.jsv.2016.01.022
3. ANSYS Swanson Analysis System, Inc., 201 Johnson Road, Houston, PA 15342/1300, USA
4. ADINA R&D, Inc. Theory and Modelling Guide. Volume I:ADINA, 2013
5. ABAQUS/CAE, Version 6.10-1, Dassault Simulia Corp. Providence, RI, USA
6. Murin J, Aminbaghai M, Hrabovsky J, Balduzzi G, Dorn M, Mang HA (2018) Torsional warping eigenmodes of FGM beams with longitudinally varying material properties. J Eng Struct 175:912–925. https://doi.org/10.1016/j.engstruct.2018.08.048
7. Rubin H (2005) Wölbkrafttorsion von Durchlaufträgern mit konstantem Querschnitt unter Berücksichtigung sekundärer Schubverformung [in German; Torsional warping theory including the secondary torsion-moment deformation-effect for beams with constant cross-section]. Stahlbau 74:826–842. https://doi.org/10.1002/stab.200590198
8. Kugler S, Fotiu PA, Murin J (2019) On the deficiences of classical theories in predicting torsional frequencies of prismatic shafts. In: In preparation for the ICOVP conference, Creette, 1–4 September, 2019
9. Murin J, Aminbaghai M, Hrabovsky J, Gogola R, Kugler S (2016) Beam finite element for modal analysis of FGM structures. Eng Struct 121:1–18 (2016). https://doi.org/10.1016/j.engstruct.2016.04.042
10. MATHEMATICA 5. Wolfram research Inc., 2003